

# Relative Mechanical Strengths of Weak Bonds in Sonochemical Polymer Mechanochemistry

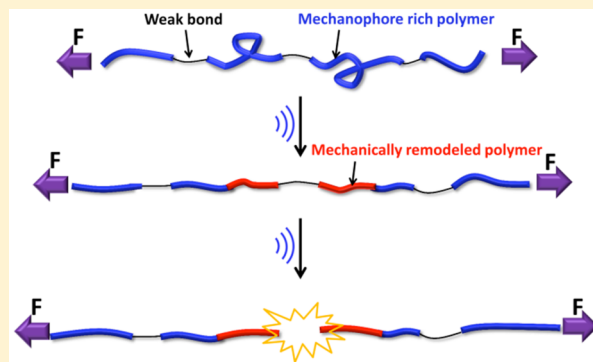
Bobin Lee,<sup>†,§</sup> Zhenbin Niu,<sup>†,§</sup> Junpeng Wang,<sup>†</sup> Carla Slebodnick,<sup>‡</sup> and Stephen L. Craig<sup>\*,†</sup>

<sup>†</sup>Department of Chemistry, Duke University, Durham, North Carolina 27708, United States

<sup>‡</sup>Department of Chemistry, Virginia Polytechnic Institute and State University, Blacksburg, Virginia 24060, United States

**S** Supporting Information

**ABSTRACT:** The mechanical strength of scissile chemical bonds plays a role in material failure and in the mechanical activation of latent reactivity, but quantitative measures of mechanical strength are rare. Here, we report the relative mechanical strength of polymers bearing three putatively “weak” scissile bonds: the carbon–nitrogen bond of an azobisdialkyl nitrile (<30 kcal mol<sup>-1</sup>), the carbon–sulfur bond of a thioether (71–74 kcal mol<sup>-1</sup>), and the carbon–oxygen bond of a benzylphenyl ether (52–54 kcal mol<sup>-1</sup>). The mechanical strengths are assessed in the context of chain scission triggered by pulsed sonication of polymer solutions, by using two complementary techniques: (i) the competition within a single polymer chain between the bond scission of interest and the nonscissile mechanochemical ring opening of *gem*-dichlorocyclopropane mechanophores and (ii) the molecular weights at long (4 h) sonication times of multimechanophore polymers. The two methods produce a consistent story: in contrast to their thermodynamic strengths, the relative mechanical strengths of the three weak bonds are azobisdialkyl nitrile (weakest) < thioether < benzylphenyl ether. The greater mechanical strength of the benzylphenyl ether relative to the thermodynamically stronger carbon–sulfur bond is ascribed to poor mechanochemical coupling, at least in part as a result of the rehybridization that accompanies carbon–oxygen bond scission.



## INTRODUCTION

Mechanically induced chemical bond scission underlies the fracture and macroscopic failure of polymeric materials, including thermosetting polymers that are widely used as rubbers and adhesives in a variety of contexts.<sup>1</sup> In addition, the mechanical scission of covalent and/or coordinative bonds can unveil latent reactivity for catalysis<sup>2</sup> or stoichiometric reactivity,<sup>3</sup> either of which can be used to create damage sensing, self-healing, and self-reinforcing materials.<sup>4</sup> Characterizing bond scission under force is therefore of considerable interest, and mechanophore scissions reported in recent years include that of a single diazo moiety in poly(ethylene glycol) (PEG),<sup>5</sup> retro-cycloadditions to unveil latent reactivity,<sup>6</sup> including remending,<sup>7</sup> the selective scission of bis-(adamantyl)-1,2-dioxetanes for mechanically triggered luminescent reporting,<sup>8</sup> and activation of latent catalysts by ligand dissociation.<sup>2,9</sup> To date, however, experimental measurements of the relative mechanical strength of the bonds that are breaking are rare.<sup>10</sup> Here, we employ the response of nonscissile *gem*-dichlorocyclopropane (gDCC) mechanophores embedded in polymers to compare the relative mechanical strengths of a series of polymers bearing presumably “weak” bonds: the carbon–nitrogen bond of an azobisdialkyl nitrile (24–30 kcal mol<sup>-1</sup>),<sup>11</sup> the carbon–sulfur bond of a thioether (71–74 kcal mol<sup>-1</sup>),<sup>12</sup> and the carbon–oxygen bond of a

benzylphenyl ether (52–54 kcal mol<sup>-1</sup>).<sup>13</sup> We find that, whereas the carbon–sulfur bond is weak and the carbon–azobond is weaker still, the benzylphenyl ether bond has a greater mechanical strength than the thioether, in contrast to their relative thermodynamic stabilities. The geometry changes that accompany rehybridization as the C–O bond breaks are implicated as a contributor to its less efficient mechanochemical coupling.

Our strategy is shown in Figure 1. The overarching idea is to exploit a competition between the activation of nonscissile mechanophores (in this case, gDCCs<sup>14</sup>) and the chain scission reaction of interest within a single polymer chain. As a polymer is trapped in the elongational flow fields that accompany the collapse of bubbles in pulsed sonication experiments, the force builds along the polymer main chain.<sup>15</sup> The force peaks near the polymer midchain and decays with distance from the peak.<sup>16</sup> This leads to mechanically triggered ring opening of the gDCC mechanophores, beginning in the center of the polymer and radiating outward in a continuous string<sup>17</sup> until the bubble collapse ends or the chain breaks. By incorporating multiple, putatively “weak”, bonds along the main chain, we set up a competition between the two mechanochemical processes of

Received: July 3, 2015

Published: August 6, 2015

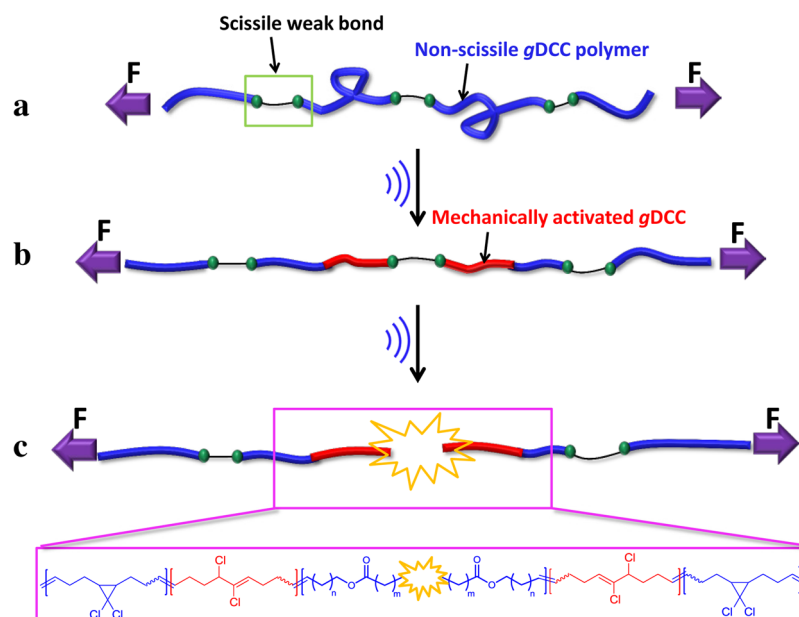


**Figure 1.** Schematic illustration of the multimechanophore approach to characterizing the strength of weak bonds. Multiple scissile bonds (thin black lines) and non-scissile mechanophores (blue) are embedded along polymer backbones (a). Elongational flow fields generated by pulsed ultrasound stretch the polymer chain (b), and the non-scissile mechanophores start to react, beginning near the midpoint of the chain and radiating outward (red), continuing until a bond breaks (c). The extent of non-scissile mechanophore activation provides a measure of the mechanical strength of the weak bond; weaker bonds break earlier, resulting in less non-scissile mechanophore activation (i.e., red area is smaller).

non-scissile gDCC ring opening and weak bond scission. The more easily the scissile bonds break, the less ring opening occurs per chain scission event, and this phenomenon has been exploited previously to discover new scissile reactions that occur between adjacent tension-trapped diradical species.<sup>18</sup> Here, we use the extent of non-scissile mechanophore activation as a measure of the relative mechanical strength of the weak bonds of interest.

## EXPERIMENTAL SECTION

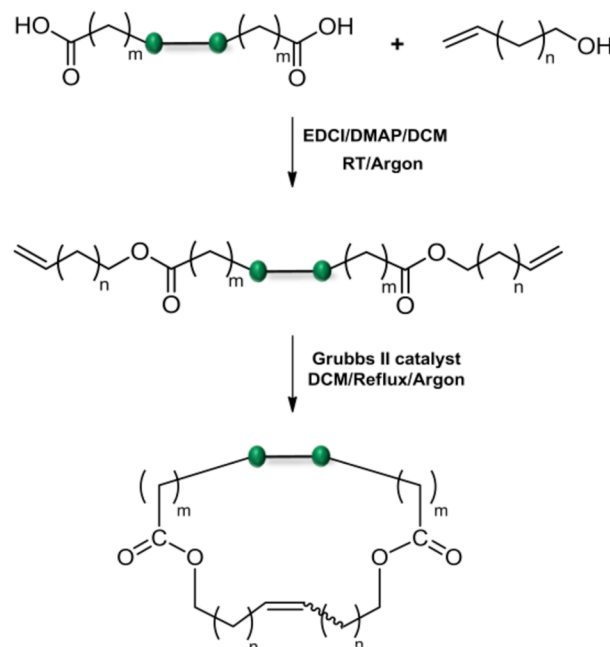
**Materials.** Dry solvents were obtained from VWR. 4,4'-Azobis(4-cyanovaleric acid), sebacic acid, 4-penten-1-ol, 3,3'-thiodipropionic acid, 5-hexen-1-ol, 1-ethyl-3-(3-(dimethylamino)propyl)-carbodiimide hydrochloride (EDCI), 4-dimethylaminopyridine (DMAP), second generation Grubbs catalyst (Grubbs II catalyst), butylated hydroxytoluene (BHT), and tetrabutyl ammonium hydroxide (TBAOH) were purchased from Sigma-Aldrich. 7-Octene-1-ol was purchased from TCI. 4-((4-Carboxybenzyl)oxy)benzoic acid,<sup>19</sup> gDCC-cyclooctadiene,<sup>20</sup> and Grubbs-py<sup>21</sup> were prepared according to procedures published previously.

**Synthesis and Characterization.** Entropy-driven ring opening metathesis copolymerization (ED-ROMP)<sup>22</sup> provides a gentle, robust, and facile methodology for embedding the necessary functionality in a quantitative manner along the polymer backbone. Weak bond mechanophores (hereafter, WBs) containing pendant bisalkenes were synthesized via mild *N*-(3-(dimethylamino)propyl)-*N*'-ethylcarbodiimide hydrochloride (EDCI)/4-(dimethylamino)pyridine (DMAP) coupling reaction. Ring closing metathesis (RCM)<sup>23</sup> of WB bisalkenes affords WB macrocyclic monomers (Scheme 1). Random copolymers (molecular weight >40 kDa) of gDCC-containing polybutadiene (PB) incorporating 11–12 mol % WB monomers were prepared via ED-ROMP with gDCC-functionalized cyclooctadiene (Scheme 2).

Since polymer mechanochemistry in pulsed ultrasound is a function of polymer contour length,<sup>14</sup> all polymers were prepared in order to have similar contour lengths (Table 1), as calculated with eq 1:

$$L_c = [(\%WB) \cdot (N_{bb}(WB)) + (1 - \%WB) \cdot (N_{bb}(gDCC))] \cdot DP \quad (1)$$

## Scheme 1. General Synthetic Approach to Weak Bond (Represented by Thin Line between Green Attachment Points) Containing Monomer for ED-ROMP



where  $L_c$  is the number of bonds along the polymer contour length, % WB is the fraction of WB repeats along the polymer backbone, DP is degree of polymerization, and  $N_{bb}$  is the number of atoms that each repeat contributes to the polymer backbone when incorporated. We use the number of bonds as a marker of contour length, as variations in the bond lengths and bond angles associated with the WB units have a negligible impact on the relative contour lengths, as compared to uncertainties in the GPC-MALS measurements.

Polymerizations were performed for relatively long times (>3 h) in order to ensure cross-metathesis and thus the formation of nearly

**Scheme 2. (a) Synthesis of Grubbs-py<sup>21</sup> and (b) General Synthetic Strategy and Naming Convention for Random Copolymers Containing Controlled Content of Weak Bonds and gDCC Mechanophores**

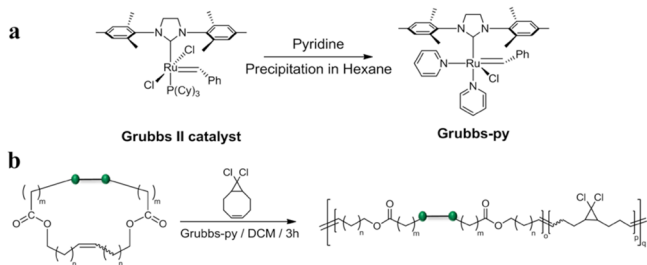
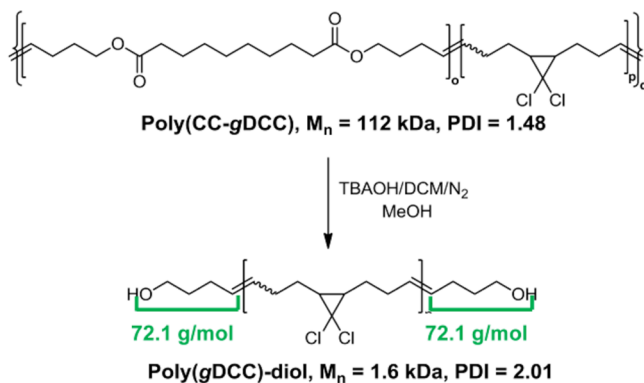


**Table 1.  $M_n$ , %WB, DP, and Calculated Contour Length ( $L_c$ ) of Polymers Employed in This Study**

	$M_n$ (kDa)	m	n	WB (mol %)		DP	$L_c$ (# atoms)
Poly(CN-gDCC)	92	2	2	12		430	4000
Poly(CS-gDCC)	97	1	3	12		470	4400
Poly(CO-gDCC)	89	0	4	11		400	3800
Poly(gDCC)	128	-	-	-	-	670	5400

random copolymers. A random copolymer structure was confirmed through methanolysis of the ester bonds in the WB repeating units. Subsequent removal of the WB fragments afforded hydroxyl-terminated poly(gDCC) fragments whose molecular weight was measured and compared to that expected for a random copolymerization. In particular, methanolysis of poly(CC-gDCC) (Scheme 3, WB =

**Scheme 3. Methanolysis of Model Copolymer to Confirm Random Copolymer Structure**



12%,  $M_n = 112$  kDa, PDI = 1.48) gave hydroxyl-terminated polymer fragments of  $M_n = 1.9$  kDa and PDI = 2.01, vs 1.9 kDa and PDI = 1.9 expected for a random copolymerization (Scheme 3, see ESI for data). In comparison, the expected  $M_n$  following methanolysis of a block copolymer is 92 kDa, and so we conclude that the copolymers have an effectively random microstructure.

These conditions were subsequently used to make the WB polymers of interest (Scheme 2): poly(CN-gDCC), carbon–nitrogen bond strength of 24–30 kcal mol<sup>-1</sup>; poly(CS-gDCC), carbon–sulfur bond strength of 71–74 kcal mol<sup>-1</sup>; and poly(CO-gDCC), carbon–oxygen bond strength of 52–54 kcal mol<sup>-1</sup>. In addition, we prepared the control polymer poly(CC-gDCC) (Scheme 3) and verified that it contains no bonds that are substantially weaker than those in the gDCC-PB portion of the polymer.

**Sonication.** The polymers were subjected to pulsed ultrasound in THF containing 3 wt % BHT at 6–9 °C in an ice–water bath under nitrogen atmosphere, and the fraction of gDCC units that underwent electrocyclic ring opening ( $\Phi$ ) was determined by <sup>1</sup>H NMR and characterized as a function of the number-averaged molecular weight ( $M_n$ ) as determined by size exclusion chromatography with multiangle light scattering (SEC-MALS).

**RESULTS AND DISCUSSION**

The effect of added WBs is often dramatic, as seen by comparing four poly(CS-gDCC) polymers with differing carbon–sulfur contents (0%, 4%, 12%, and 15%). As the carbon–sulfur content increases, the rate of molecular weight degradation increases (Figure 2a), and the fraction of gDCC

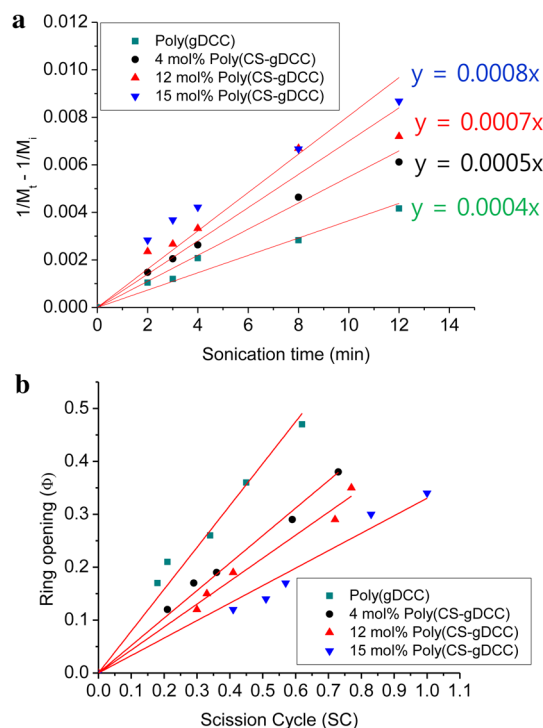


**Figure 2.** (a) Relative rates of sonochemical polymer scission of poly(gDCC) as a function of carbon–sulfur bond content. (b) Fraction of ring opening of gDCC mechanophores as a function of scission cycle and carbon–sulfur content. Red lines represent linear fits to data points constrained through the origin; slope =  $\Phi_i$ .

ring opening,  $\Phi$ , also increases as a function of scission cycle<sup>18</sup> (SC, where  $SC = [\ln(M_{n,0}) - \ln(M_{n,t})]/\ln 2$ ; Figure 2b). For convenience, we report the competition between gDCC ring opening and chain scission in terms of  $\Phi_i$ , the initial slope of the  $\Phi$  vs SC curve. Whereas  $\Phi_i = 0.79$  for poly(gDCC), it drops to 0.52, 0.43, and 0.33 for carbon–sulfur monomer contents of 4%, 12%, and 15%, respectively. That the reduction in  $\Phi_i$  is due to the carbon–sulfur, rather than some other bond, is confirmed by sonicating the control poly(CC-gDCC), whose  $\Phi_i$  is indistinguishable from that of poly(gDCC) (see ESI, Table S4). In addition to confirming that WB content drives  $\Phi_i$ , these results also provide limits on the effect of small variations in WB content on experimental  $\Phi_i$  values. The differences in  $\Phi_i$  between different WB polymers (see below) are greater than can be ascribed to the  $\pm 1\%$  variation in WB content.

The thermodynamic strength of the carbon–nitrogen bond in the azobisdialkyl nitrile mechanophores exploited previously

by Moore and co-workers<sup>5</sup> is weaker than the carbon–sulfur bond, and so we expected its mechanical strength to be lower as well. Consistent with this expectation,  $\Phi_i$  of poly(CN-gDCC) with 12% WB was found to be 0.18, less than the corresponding poly(CS-gDCC). The azobisdialkyl nitriles are therefore not only highly efficient thermally triggered initiators of free radical chemistry but highly efficient mechanochemically triggered initiators as well. In fact, the forces necessary for their activation in the ultrasound experiments are apparently comparable to those required to open the gDCC mechanophores themselves ( $\sim 2$  nN in this context; see below).<sup>24</sup>

By comparison, the relative strength of poly(CO-gDCC) was initially something of a surprise to us, as its  $\Phi_i$  of 0.62 is higher than that of poly(CS-gDCC), despite the fact that the homolytic bond dissociation energy of its carbon–oxygen bond ( $S_2$ – $S_4$  kcal mol<sup>-1</sup>) is lower than that in the carbon–sulfur units. In fact, the behavior is closer to that of the control polymers (Figure 3). The benzylphenyl ether unit therefore exhibits disproportionately high mechanical stability given its relatively modest thermodynamic stability.

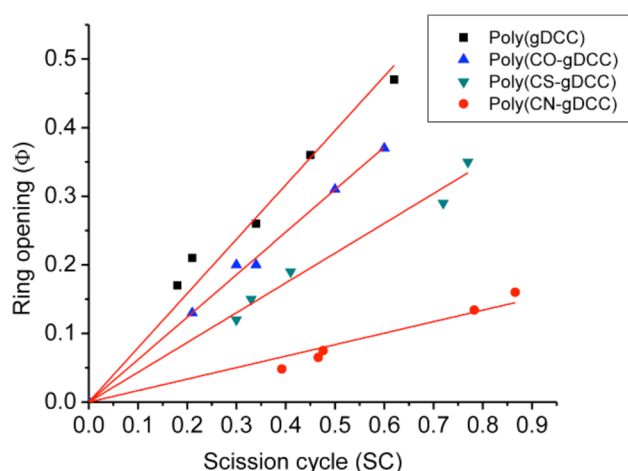


**Figure 3.** Ring opening ( $\Phi$ ) as a function of scission cycle (SC) in three putative weak bond containing polymers and two control polymers. Red lines are linear fits to the data constrained through the origin; slope =  $\Phi_i$ .

We attribute the relative lack of mechanochemical activity in the benzyl ether to poor mechanochemical coupling due to at least in part to rehybridization during the bond dissociation. A primary factor contributing to the low thermodynamic bond strength is the differential resonance stabilization of the benzyl radical that is formed upon scission. The resonance stabilization involves a formal rehybridization of the benzyl carbon atom upon which unpaired spin is concentrated, from  $sp^3$  to  $sp^2$ , and the associated geometry changes develop smoothly as the carbon–oxygen bond lengthens. As a result, the length gained across the mechanophore as the C–O distance increases is partially offset by the contraction that results as the C(phenyl)–C(benzyl)–O bond angle decreases, from close to  $109^\circ$  toward  $90^\circ$ , in order to accommodate the rehybridization. It is the overall change in length across all coupled nuclei that dictates mechanochemical coupling, and such effects have been shown to have substantial impact on mechanophore activity.<sup>24,25</sup> As shown in Figure 4, the end-to-end distance of the benzylphenyl ether changes almost insignificantly ( $0.035$  Å) when the C–O bond is computationally

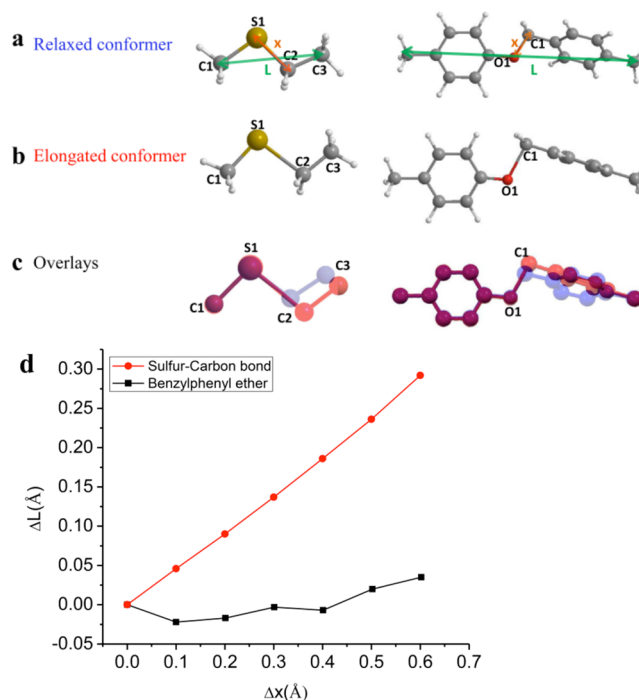


**Figure 4.** (a) Calculated original geometries of ethylmethyl thioether (left) and benzylphenyl ether (right). (b) Calculated geometries for the same molecules in which the S1–C2 (left) and C1–O1 (right) distances are constrained to be  $0.6$  Å longer than their initial values. (c) Overlay of initial (blue) and constrained (red) geometries from (a) and (b), respectively. (d) Plot of change in overall length ( $\Delta L$ ) as a function of change in central bond length ( $\Delta x$ ).

stretched by  $0.6$  Å, as opposed to a distinct offset of  $0.292$  Å calculated for the carbon–sulfur distance (see ESI for computational details), and differences in coupling are observed across all bond extensions. The consequences of secondary structural changes, including those involving rehybridization, in the context of mechanochemical coupling were first proposed by Boulatov<sup>26</sup> to account for a lack of force dependence observed in the nucleophilic exchange of disulfides embedded within highly strained macrocycles, to which the explanation offered here is quite similar.

The measured  $\Phi_i$  values describe the amount of ring opening that accompanies a representative single bond scission, and they can be related to quantitative models of the force distribution along the polymer backbone during elongational flow. For fully extended polymer chains, the force distribution is parabolic (Figure 5) with a peak force ( $F_{\text{break}}$ ) that corresponds to the average force necessary to break a covalent bond on the time scale of the extension event. In this limit, the fraction of the polymer chain,  $\Phi$ , that experiences a force sufficient for ring opening ( $F_{\text{open}}$ ) is given by

$$\Phi = ((F_{\text{break}} - F_{\text{open}})/F_{\text{break}})^{1/2} \quad (3)$$

The relevant time scale for the extension is taken here to be  $10^{-6}$  s, and extrapolating our previous force spectroscopy studies<sup>24</sup> to that time scale gives  $F_{\text{open}} = 2040$  pN for the *gem*-dichlorocyclopropanes. For simplicity, we assume that the competition between ring opening and chain scission represents the average behavior of a single chain that it stretched to the point of scission. Setting  $\Phi = \Phi_i = 0.79 \pm 0.03$ , the corresponding value of  $F_{\text{break}}$  for the poly(gDCC) backbone is  $5.4 \pm 0.7$  nN. While certainly not precise given the

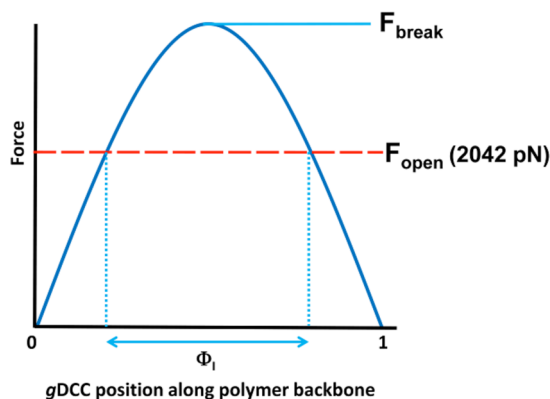


**Figure 5.** Theoretical force distribution along a polymer backbone under the extensional flows generated by pulsed ultrasound.  $F_{\text{break}}$  represents the average force at which the polymer chain breaks.  $F_{\text{open}}$  represents the force required for gDCC activation on the characteristic time scale of the extensional flow field. The  $x$ -axis range subsumed by the points at which the graph crosses  $F_{\text{open}}$  gives  $\Phi_i$ . The general shape of the distribution is fixed, and so as  $F_{\text{break}}$  increases, the fraction of the distribution that exceeds  $F_{\text{open}}$  increases as well, leading to higher values of  $\Phi_i$ .

approximations involved, this value is nonetheless reasonable as a rough quantitative benchmark, and it compares well to a force of  $\sim 5$  nN calculated by Beyer for rupture of a typical carbon-carbon bond on  $10^{-6}$  s time scales<sup>27</sup> and extrapolated by Lebedeva and co-workers for the scission of adsorbed bottlebrush polymers (by comparison  $F_{\text{break}} = 5$  nN corresponds to an expected  $\Phi = 0.77$ ).<sup>28</sup> The calculated peak force for poly(CO-gDCC), in comparison, is 3.3 nN, and that derived for poly(CS-gDCC) is 2.5 nN. We regard these numbers as reasonable estimates, but their accuracy assumes that the polymer chains are fully stretched<sup>29</sup> and that both activation without scission (which would artificially increase  $\Phi$ ) and multiple scissions of a single chain (which would artificially lower it) are rare events. We note in particular that multiple scissions of a single parent chain (and perhaps incomplete uncoiling) are increasingly likely for weaker bonds, and so the observed  $\Phi_i$  values of poly(CN-gDCC) likely underreport the true mechanical strength of those bonds relative to the other mechanophores.

Under pulsed ultrasound, polymer chains are broken more rapidly for the polymers having higher molecular weight. As polymer molecular weight decreases due to scission, chain scission slows down considerably because it is difficult for shorter chains to achieve the required force.<sup>1,30</sup> Under our conditions, 4 h of sonication is sufficient to reach molecular weights that change only very slowly with additional sonication. We refer to the molecular weight after 4 h of sonication as  $M_{4\text{h}}$ . The more easily the polymer chain breaks, the lower the  $M_{4\text{h}}$  is expected to be. Thus,  $M_{4\text{h}}$  should also be indicative of the mechanical strengths of bonds that are incorporated into a polymer chain, as described by Sijbesma and co-workers in their study of silver coordination polymers.<sup>31</sup> The expected relationship holds in the polymers studied here, as  $M_{4\text{h}}$  and  $\Phi_i$  show the same trends in relative mechanical strength (Table 2).

The observed relationship between  $M_{4\text{h}}$  and  $\Phi_i$  is quantitatively reasonable, as well. The forces at break,  $F_{\text{break}}$ , derived from  $\Phi_i$  using eq 3 should be reasonable estimates of the average maximum forces experienced on the time scale of the ongoing sonication at which  $M_{4\text{h}}$  is reached. Because the

**Table 2.**  $\Phi_i$ , Molecular Weight after 4 h of Sonication ( $M_{4\text{h}}$ ) and Calculated  $F_{\text{break}}$  Using  $\Phi_i$  of Each Polymer

polymer	$\Phi_i$	$M_{4\text{h}}$ (kDa)	$F_{\text{break}}$ (nN)
poly(gDCC)	0.79	28.3	5.4
poly(CO-gDCC)	0.62	22.8	3.3
poly(CS-gDCC)	0.43	19.3	2.5
poly(CN-gDCC)	0.18	15.3	2.1

maximum theoretical force experienced by a polymer chain in an elongational flow field goes with the square of polymer contour length,<sup>31,32</sup> we expect a power law dependence between  $F_{\text{break}}$  calculated as above and  $M_{4\text{h}}$  given by eq 4:

$$F_{\text{break}} = C(M_{4\text{h}})^2 \quad (4)$$

As seen in Figure 6, the observed power law dependence across all data is 1.5. We note that poly(CN-gDCC) is

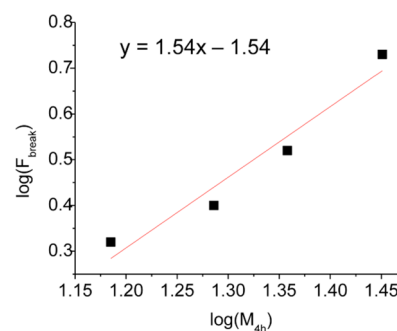


**Figure 6.** log–log plot of  $F_{\text{break}}$  vs  $M_{4\text{h}}$  showing scaling exponent of 1.5.

somewhat of an outlier from the remaining polymers, not surprising because: (i) the relative mechanical activity of the scissile and nonscissile mechanophores means that the extent of nonscissile activation might be more sensitive to the exact location of scissile mechanophores within an individual polymer chain, (ii) the probability of gDCC activation without scission is negligible, and (iii) the moderate thermal stability of the diazo linkage might lead to contributions from force-free scission that are not present in the other polymers. Notably, when poly(CN-gDCC) is omitted from the fit, the observed power law dependence of the remaining three polymers is 2.0, as expected from eq 4. Given the assumptions involved in calculating  $F_{\text{break}}$ , this result is likely fortuitous, but the analysis supports that the expected physical picture is likely at play and also supports that reasonable quantitative estimates of the mechanical strengths of scissile bonds can be drawn from sonication experiments.

## CONCLUSION

The results demonstrate the utility of nonscissile, multi-mechanophore polymers as reporters of the relative mechanical strength of weak scissile bonds embedded within them. The competition between scissile and nonscissile processes reveals that azobisdialkyl nitriles are activated at lower forces than thioethers and benzylphenyl ethers, although the latter are still much weaker than the rest of a polybutadiene-based polymer backbone. The benzylphenyl ethers are much less mechanically susceptible than would be expected from a thermodynamic bond strength that is lower than that of the thioether. As has been emphasized in recent publications,<sup>24–26</sup> the importance of considering geometry changes beyond those associated with the

local motions of nuclei involved directly in bond making/breaking is seen to be a critical design element through which the mechanical and thermal stability of reagents might be manipulated independently.

The methodologies employed have advantages in that they are relatively simple to apply and generate data that are amenable to quantitative treatments. Because the key results in the case of the non-scissile mechanophore reporters involve an internal competition, the approach might also require fewer experiments and be less susceptible to slight day-to-day variations, such as those due to changes in sonication power, than are extrapolated rate measurements that have been applied successfully to other scissile mechanophores.<sup>6</sup> The use of “near-limiting” molecular weights, on the other hand, is even simpler to apply as long as all experiments can be done under very similar conditions. We see no reason that both approaches should not be applicable to any scissile process, so long as the “weak bond” in question is both strong enough to withstand the forces necessary to open the non-scissile mechanophore reporters and weak enough that it can be distinguished from the control polymer.

As implemented here, both approaches provide good quantitative measures of relative mechanical bond strength under pulsed sonication conditions. While the estimates of absolute mechanical bond strengths are likely reasonable, the accuracy of those values will be improved by a better understanding of the effect of mechanophore content and distribution, as well as polymer molecular weight and dispersity, on both scissile and non-scissile mechanophore activation. Dynamics, both of reactions under high forces and of polymer chain extension under high strain rate elongational flow fields, might also play a role.

## ■ ASSOCIATED CONTENT

### 📄 Supporting Information

The Supporting Information is available free of charge on the ACS Publications website at DOI: 10.1021/jacs.5b06937.

Details of syntheses, characterization data, NMR spectra, GPC analysis result, crystal cif files, and details of calculation (PDF)

## ■ AUTHOR INFORMATION

### Corresponding Author

\*E-mail: [Stephen.Craig@duke.edu](mailto:Stephen.Craig@duke.edu).

### Author Contributions

<sup>§</sup>B.L. and Z.N. contributed equally.

### Notes

The authors declare no competing financial interest.

## ■ ACKNOWLEDGMENTS

This material is based on work supported by the NSF (CHE-1508566) and NSF MIRT (DMR-1122483).

## ■ REFERENCES

- (1) Caruso, M. M.; Davis, D. A.; Shen, Q.; Odom, S. A.; Sottos, N. R.; White, S. R.; Moore, J. S. *Chem. Rev.* **2009**, *109*, 5755.
- (2) (a) Piermattei, A.; Karthikeyan, S.; Sijbesma, R. P. *Nat. Chem.* **2009**, *1*, 133. (b) Jakobs, R. T. M.; Sijbesma, R. P. *Organometallics* **2012**, *31*, 2476.
- (3) Groote, R.; van Haandel, L.; Sijbesma, R. P. *J. Polym. Sci., Part A: Polym. Chem.* **2012**, *50*, 4929.

- (4) (a) Ramirez, A. L. B.; Kean, Z. S.; Orlicki, J. A.; Champhekar, M.; Elsakar, S. M.; Krause, W. E.; Craig, S. L. *Nat. Chem.* **2013**, *5*, 757. (b) Davis, D. A.; Hamilton, A.; Yang, J.; Cremer, L. D.; Van Gough, D.; Potisek, S. L.; Ong, M. T.; Braun, P. V.; Martinez, T. J.; White, S. R.; Moore, J. S.; Sottos, N. R. *Nature* **2009**, *459*, 68. (c) Diesendruck, C. E.; Moore, J. S. In *Self-Healing Polymers*; Binder, W. H., Ed.; Wiley-VCH Verlag GmbH & Co. KGaA: Weinheim, Germany, 2013.
- (5) Berkowski, K. L.; Potisek, S. L.; Hickenboth, C. R.; Moore, J. S. *Macromolecules* **2005**, *38*, 8975.
- (6) Kryger, M. J.; Munaretto, A. M.; Moore, J. S. *J. Am. Chem. Soc.* **2011**, *133*, 18992.
- (7) Klukovich, H. M.; Kean, Z. S.; Iacono, S. T.; Craig, S. L. *J. Am. Chem. Soc.* **2011**, *133*, 17882.
- (8) Chen, Y. L.; Spiering, A. J. H.; Karthikeyan, S.; Peters, G. W. M.; Meijer, E. W.; Sijbesma, R. P. *Nat. Chem.* **2012**, *4*, 559.
- (9) Groote, R.; Jakobs, R. T. M.; Sijbesma, R. P. *ACS Macro Lett.* **2012**, *1*, 1012.
- (10) (a) Park, I.; Sheiko, S. S.; Nese, A.; Matyjaszewski, K. *Macromolecules* **2009**, *42*, 1805. (b) Sheiko, S. S.; Sun, F. C.; Randall, A.; Shirvanyants, D.; Rubinstein, M.; Lee, H.-i.; Matyjaszewski, K. *Nature* **2006**, *440*, 191. (c) Beyer, M. K.; Clausen-Schaumann, H. *Chem. Rev.* **2005**, *105*, 2921.
- (11) Sun, C.; Zhao, H.; Fang, D.; Li, Z. *J. Mol. Struct.: THEOCHEM* **2004**, *679*, 89.
- (12) (a) Hawari, J. A.; Griller, D.; Lossing, F. P. *J. Am. Chem. Soc.* **1986**, *108*, 3273. (b) Nicovich, J. M.; Kreutter, K. D.; Van Dijk, C. A.; Wine, P. H. *J. Phys. Chem.* **1992**, *96*, 2518.
- (13) (a) Matsunaga, N.; Rogers, D. W.; Zavitsas, A. A. *J. Org. Chem.* **2003**, *68*, 3158. (b) Pratt, D. A.; de Heer, M. I.; Mulder, P.; Ingold, K. U. *J. Am. Chem. Soc.* **2001**, *123*, 5518.
- (14) Lenhardt, J. M.; Black, A. L.; Craig, S. L. *J. Am. Chem. Soc.* **2009**, *131*, 10818.
- (15) (a) Caruso, M. M.; Davis, D. A.; Shen, Q.; Odom, S. A.; Sottos, N. R.; White, S. R.; Moore, J. S. *Chem. Rev.* **2009**, *109*, 5755. (b) Paulusse, J. M. J.; Sijbesma, R. P. *J. Polym. Sci., Part A: Polym. Chem.* **2006**, *44*, 5445.
- (16) Odell, J. A.; Keller, A. *J. Polym. Sci., Part B: Polym. Phys.* **1986**, *24*, 1889.
- (17) Black Ramirez, A. L.; Ogle, J. W.; Schmitt, A. L.; Lenhardt, J. M.; Cashion, M. P.; Mahanthappa, M. K.; Craig, S. L. *ACS Macro Lett.* **2012**, *1*, 23.
- (18) Lenhardt, J. M.; Ogle, J. W.; Ong, M. T.; Choe, R.; Martinez, T. J.; Craig, S. L. *J. Am. Chem. Soc.* **2011**, *133*, 3222.
- (19) Lan, Y.-Q.; Li, S.-L.; Qin, J.-S.; Du, D.-Y.; Wang, X.-L.; Su, Z.-M.; Fu, Q. *Inorg. Chem.* **2008**, *47*, 10600.
- (20) Okazaki, R.; Ooka, M.; Tokitoh, N.; Inamoto, N. *J. Org. Chem.* **1985**, *50*, 180.
- (21) Sanford, M. S.; Love, J. A.; Grubbs, R. H. *Organometallics* **2001**, *20*, 5314.
- (22) (a) Hodge, P.; Kamau, S. D. *Angew. Chem., Int. Ed.* **2003**, *42*, 2412. (b) Kamau, S. D.; Hodge, P.; Hall, A. J.; Dad, S.; Ben-Haida, A. *Polymer* **2007**, *48*, 6808. (c) Tastard, C. Y.; Hodge, P.; Ben-Haida, A.; Dobinson, M. *React. Funct. Polym.* **2006**, *66*, 93.
- (23) Lee, C. W.; Grubbs, R. H. *Org. Lett.* **2000**, *2*, 2145.
- (24) Klukovich, H. M.; Kouznetsova, T. B.; Kean, Z. S.; Lenhardt, J. M.; Craig, S. L. *Nat. Chem.* **2012**, *5*, 110.
- (25) Groote, R.; Szyja, B. M.; Leibfarth, F. A.; Hawker, C. J.; Doltsinis, N. L.; Sijbesma, R. P. *Macromolecules* **2014**, *47*, 1187.
- (26) Kucharski, T. J.; Huang, Z.; Yang, Q. Z.; Tian, Y. C.; Rubin, N. C.; Concepcion, C. D.; Boulatov, R. *Angew. Chem., Int. Ed.* **2009**, *48*, 7040.
- (27) Beyer, M. K. *J. Chem. Phys.* **2000**, *112*, 7307.
- (28) Lebedeva, N. V.; Nese, A.; Sun, F. C.; Matyjaszewski, K.; Sheiko, S. S. *Proc. Natl. Acad. Sci. U. S. A.* **2012**, *109*, 9276.
- (29) Perkins, T. T.; Smith, D. E.; Chu, S. *Science* **1997**, *276*, 2016.
- (30) Price, G. J.; Smith, P. F. *Polymer* **1993**, *34*, 4111.
- (31) Groote, R.; Szyja, B. M.; Pidko, E. A.; Hensen, E. J. M.; Sijbesma, R. P. *Macromolecules* **2011**, *44*, 9187.

(32) (a) Kuijpers, M. W. A.; Iedema, P. D.; Kemmere, M. F.; Keurentjes, J. T. F. *Polymer* **2004**, *45*, 6461. (b) Müller, A. J.; Odell, J. A.; Carrington, S. *Polymer* **1992**, *33*, 2598. (c) Odell, J. A.; Keller, A. J. *Polym. Sci., Part B: Polym. Phys.* **1986**, *24*, 1889. (d) Nguyen, T.; Kausch, H.-H. In *Macromolecules: Synthesis, Order and Advanced Properties*; Springer: Berlin, 1992; Vol. 100/1.